ELSEVIER

www.elsevier.nl/locate/jorganchem

Journal of Organometallic Chemistry 616 (2000) 1–9

Journal of Organometallic Chemistry

Analysis of the vibrational spectra, force fields, and molecular structures of pentacarbonyl(methyl)manganese(I) and pentacarbonyl(methyl)rhenium(I)

É. Bencze [a,*], J. Mink [a,b], I. Pápai [a], I.S. Butler [c], D. Lafleur [c], D.F.R. Gilson [c]

[a] *Institute of Isotope and Surface Chemistry, Chemical Research Center, Hungarian Academy of Sciences, P.O.B. 77, H-1525 Budapest, Hungary*

[b] *Department of Analytical Chemistry, University of Veszprém, P.O.B. 158, H-8201 Veszprém, Hungary*

[c] *Department of Chemistry, McGill University, 801 Sherbrooke St. West, Montreal, Quebec, Canada H3A 2K6*

Received 10 April 2000

Abstract

Vibrational spectra of $CH_3Mn(CO)_5$ and $CH_3Re(CO)_5$ have been reinvestigated in particular in the far-IR (500–50 cm^{-1}) region. Raman (3500–50 cm^{-1}) solid phase (at ambient and liquid nitrogen temperature) and solution (in CH_2Cl_2) polarization data for the Re compound are presented. Based on the available and the present experimental data and the results of the normal coordinate calculations, the assignment of the frequencies has been reviewed and some modifications in the low frequency region have been suggested. Force-field calculations have been performed on the basis of vibrational data of the $-CH_3$, $-CD_3$, and $-^{13}CH_3$ species of gaseous, dissolved, and solid samples. Density functional theory calculations show that the rotational barrier of the methyl group is less than 0.5 kcal mol^{-1}. The study of pressure effect on CO and M–CH_3 stretching force constants proved that the stronger CO bonds have a relatively smaller pressure effect than the much weaker M–CH_3 bonds. As a characteristic of pressure sensitivity 'bond compressibility' has been introduced.

Keywords: Manganese and rhenium; FTIR; FT-Raman spectroscopy; Normal coordinate analysis; Density functional theory

1. Introduction

Earlier studies of the IR and Raman spectra of the well-known metal-alkyl complex, $CH_3Mn(CO)_5$, have dealt chiefly with the CO and CH_3 stretching [1–7] and the low-frequency regions [8]. Subsequent vibrational work on both $CH_3Mn(CO)_5$ and the analogous rhenium complex, $CH_3Re(CO)_5$ [9–14] including an examination of the effects of high external pressures [11], attest to the continued interest in these relatively simple molecules. The local symmetries of the CH_3M- and $-M(CO)_5$ moieties are C_{3v} and C_{4v}, respectively. Detailed force-field calculations (for only the totally-symmetric modes however) have been undertaken by using frequency data for the gaseous $-CH_3$, $-CD_3$, and $-^{13}CH_3$ species [10]. Also, an energy-factored force field has been calculated for the CO stretching modes by using gas phase [10] and matrix isolation [13] data. An interesting feature of the $CH_3M(CO)_5$ (M = Mn, Re) molecules is whether or not the CH_3 groups are freely rotating with respect to the $-M(CO)_5$ moieties or they are rotationally hindered [8–10,14,15].

Despite the considerable attention already paid to the vibrational spectra of the $CH_3M(CO)_5$ (M = Mn, Re) molecules, the analyses are by no means complete. In particular, there are relatively few Raman spectral data available, especially for the rhenium compound, and surprisingly no far-IR spectra have been reported for the title compounds. Moreover, calculation of the full force fields for the gaseous, dissolved, and solid samples is necessary if realistic bonding comparisons are to be made, particularly with related metal pentacarbonyl derivatives such as $Mn(CO)_5Br$ [17] and $[Cr(CO)_5CN]^-$ [18], for which complete force field calculations are available.

* Corresponding author. Tel./fax: +36-1-3922551.
E-mail address: mink@iserv.iki.kfki.hu (É. Bencze).

0022-328X/00/$ - see front matter
PII: S0022-328X(00)00512-X

In view of the reasons cited above, we decided to undertake a detailed vibrational study of the $CH_3M(CO)_5$ (M = Mn, Re) complexes, including a 'complete' force-field calculation for such molecules.

2. Experimental

2.1. Materials

The $CH_3M(CO)_5$ (M = Mn [19], Re [20]) complexes were prepared and purified by the literature methods indicated. The solvents used were of spectrograde quality.

2.2. Instrumentation

Mid- and far-IR spectra were recorded at 2 cm^{-1} resolution on a BIO-RAD Digilab FTS-60A system and a BIO-RAD Digilab FTS-40 spectrometer, respectively. Solid samples were studied as mulls in heavy liquid paraffin–vaseline mixtures or pressed in polyethylene pellets. Solution IR measurements (in CS_2 and CH_2Cl_2, respectively) were made using KBr cells (0.1- or 0.2-mm pathlength).

Raman spectra were recorded on an Instruments S.A. U-1000 Ramanor spectrometer interfaced to a computer. The excitation source was the 514.5-nm line of a Spectra-Physics model 164 5-W argon-ion laser. The solids were examined as ground powders in melting-point capillary tubes. Solutions (in CH_2Cl_2) were studied in a 1.0-cm quartz cell fitted with parallel optical windows. For determination of the depolarization ratios, the integrated band intensities were used. The resolution employed was typically 2 cm^{-1}. Low-temperature Raman spectra were recorded with the aid of a Cryogenics cryostat. Some of the Raman spectra of solids were made with a BIO-RAD dedicated FT-Raman spectrometer using a Nd–YAG laser. The laser power at the sample was $\sim$150 mW.

Table 1
Far-IR data for solid $CH_3M(CO)_5$ (M = Mn, Re) complexes (cm^{-1})

$CH_3Mn(CO)_5$	$CH_3Re(CO)_5$	Assignment		
550 vw	488 vw	ν_{23}	e	MCO_a bend.
497 w	471 vw	ν_6	a_1	M–CO_a str.
463 vs	381 vs	ν_{24}	e	M–CO_e str.
440 wm	434 w	ν_{25}	e	M–CO_e oop. def.
422 vvw	418 vvw	ν_{14}	b_1	M–CO_e str.
420 w	447 m	ν_7	a_1	M–CH_3 str.
406 w	447 m	ν_8	a_1	M–CO_e str.
164 w	140 vw	ν_{26}	e	CMC def.
112 w	105 vw, b	ν_{15}	b_1	CMC def.
92 w	95 w, b	ν_9, ν_{27}	a_1, e	CMC def., CMC def.
[70] [a]	[60] [a]	ν_{28}	e	CMC def.

[a] Estimated frequencies.

2.3. Force-field calculations

Since the fundamentals differ quite significantly for the gases compared to those for the dissolved and solid states, we have calculated force constants for all three sets of frequencies. The geometrical parameters used in the calculations were taken from Refs. [19,20]. The standard GF matrix method was used to solve the secular equation for which G matrices were calculated by a computer program described earlier [21].

Initial force constants were taken from CH_3HgX [22] for the CH_3 group and from $Mn(CO)_5Br$ [17] for the $-M(CO)_5$ moiety. There are 39 fundamentals for $CH_3Mn(CO)_5$, $CD_3Mn(CO)_5$ and their methyl ^{13}C-labelled species. We have refined 31 force constants which included all the diagonal force constants, seven stretch–stretch interaction constants, and four stretch–bend cross terms. The other 49 non-diagonal force constants were constrained to the values of CH_3HgX [22] and $Mn(CO)_5Br$ [17]. The force fields of both $CH_3Mn(CO)_5$ and $CH_3Re(CO)_5$ were refined with identical constraints in each case. The refinement procedure was repeated for the gas, solution, and solid-state sets of frequencies.

2.4. Density functional theory (DFT) calculations

These were carried out at the nonlocal level of theory using the BP86 functional [23,24]. The (63321/5211/41) (for Mn) [25], (5211/411/1) (for C and O) [26] and (41/1) (for H) [26] orbital basis sets were used within the LCGTO-DF formalism [27] as implemented in the DEMON program package [28,29]. The technical details of the calculations are identical to those in Ref. [30].

3. Results

3.1. Vibrational assignments and selection of fundamentals

3.1.1. $CH_3Mn(CO)_5$

The available literature data for this complex were almost sufficient to provide fundamental frequencies for force constant calculations for the gas, solution, and solid samples. We collected the missing far-IR spectra of solid $CH_3Mn(CO)_5$ (Table 1) and to improve the assignments we repeated the Raman measurements of the solid at room temperature and at 58 K.

We basically accepted the assignments proposed by Andrews et al. [8], and McQuillan and his co-workers [10], except that the solution polarization data were rather incomplete and in some cases we disagreed with those reported by the former groups. The ν_1 and ν_2 bands fall close to each other in solution and in the solid state for the $CD_3Mn(CO)_5$ species. Since ν_2 shows no deuterium sensitivity, it should appear in the 2125–

2110 cm^{-1} range, and probably in solution the ν_1 band is also in this region. Our estimated frequencies for these are $\nu_1 \cong \nu_2 \cong 2116$ cm^{-1}. The ν_{21} mode in gaseous $CH_3Mn(CO)_5$ was originally assigned to a band at 755 cm^{-1}, which we find too low when compared to 789 and 784.5 cm^{-1} for the solution and solid, respectively. Our estimated frequency is 805 cm^{-1} which matches the gas/solid frequency shift observed for the 599.5/584.5 cm^{-1} bands of $CD_3Mn(CO)_5$. All the bands associated with the ν_6, ν_7, ν_8, ν_{14}, ν_{24}, and ν_{25} modes are expected to appear in the 500–400 cm^{-1} range. There are three polarized bands in this region. The more ^{13}C and CD_3 sensitive is the Mn–CH_3 stretching mode ν_7, while another is the Mn–CO_e stretching of the equatorial CO groups, ν_8. The weak Raman band at 490 cm^{-1} which is probably polarized can be assigned to ν_6 (Mn–CO_a stretching of the axial CO group) on the argument that ν_6 should be higher in energy than is ν_8. The ν_6 band is listed in Andrews et al.'s paper as being depolarized, while the extremely weak band at 561 cm^{-1}, which is difficult to measure, is given as polarized. The strong IR band at $\sim$460 cm^{-1}, the medium band at $\sim$440 cm^{-1}, and the weak band at $\sim$420 cm^{-1} have been assigned to ν_{24}, ν_{25}, and ν_{14}, respectively. The ν_{24} mode is detected in the solution Raman spectrum as a shoulder. The ν_{25} and ν_{24} modes are overlapped with the strong and broad polarized ν_7 and ν_8 bands. The positions of the inactive a_2 mode (ν_{10}) and the very low frequency ν_{28} band can be predicted from combination frequencies (374 and 70 cm^{-1}, respectively).

3.1.2. $CH_3Re(CO)_5$

The vibrational spectra of the rhenium compound have been less studied than is the case for the manganese analogue. No solution spectra and no far-IR spectra have been reported. Raman spectra of solid $CH_3Re(CO)_5$ and of its $-^{13}CH_3$ and $-CD_3$ derivatives have been measured only in the 600–300 cm^{-1} region [10]. The far-IR and Raman frequencies observed by us are presented in Tables 1 and 2, respectively, while representative IR and Raman spectra of CH_2Cl_2 solution in the CO stretching region are shown in Fig. 1. Only the strongest Raman band at 2129 cm^{-1} was found to be polarized and the ν_3 CO_a stretching mode is depolarized. Another point that should be noticed is that the weak IR band at 2044 cm^{-1} is probably not the appearance of the IR-inactive b_1 mode (ν_{12}), as indicated by McQuillan et al., but it is more likely a combination mode because the strong ν_{12} Raman band is observed at higher energy (2052 cm^{-1}).

Assignment of the vibrational spectra below 700 cm^{-1} basically agreed with the previous study [10] except the band at $\sim$500 cm^{-1}, which we assign as ν_{23} based on potential energy distribution (PED) rather than a combination band. Only two polarized Raman lines were observed in this region (see Table 2), which can be attributed to the ν_6 (470 cm^{-1}) and ν_7 (450 cm^{-1}) modes. The latter showed $^{13}CH_3$ and CD_3 sensitivity [10]. No other bands near 450 cm^{-1} have been observed; therefore, it is reasonable to assign ν_8 (Re–CO_e) to the same frequency. The assignment of the ν_{14} mode is still uncertain. We have completed the spectrum assignment by measuring some important low-frequency fundamentals below 200 cm^{-1} (see Table 2).

4. Discussion

The agreement between the experimental and calculated frequencies for the gaseous molecules is very good. The deviations between them are generally below 2%, with the exception of the modes located about 100 cm^{-1} and below. Rather large deviations in absolute values are observed for ν_1 which are presumably due to the anharmonicities of the observed symmetric CH and CD stretching modes. It is interesting to note that vibrations of b_1 and b_2 symmetry do not show any isotopic sensitivity with isotope substitution of the CH_3 group.

As mentioned in Section 1, it has been shown by different spectroscopic methods that the CH_3 groups are freely rotating with respect to the $-M(CO)_5$ moieties [8–10,14,15]. In our work, there are other experimental observations which lead us to suspect free rotation of the C_{3v} methyl group with respect to the C_{4v} pentacarbonyl skeleton:

1. The vibrational spectra of these compounds display practically no vibrational coupling between the $-CH_3$ and $-M(CO)_5$ moieties since no CH_3/CD_3 isotope effects are observed for any of the CO stretching modes and for all modes of b_1 and b_2 symmetry.
2. According to the calculated PED data and to the eigenvectors of the modes, there is no real mixing of vibrational coordinates between the $-CH_3$ and $-M(CO)_5$ moieties. No vibrational coupling was observed for the b_1 and b_2 modes and practically no or negligible interactions were found for the e species. Some interaction between the coordinates of the $-CH_3$ and $-M(CO)_5$ moieties have been observed for a_1 species, basically via the M–CH_3 stretching coordinate (R). This metal–carbon mode (ν_7) interacts with other vibrations such as ν_4, ν_6 and ν_8.

In an attempt to estimate the energy barrier of the CH_3 internal rotation, we have carried out DFT calculations for the $CH_3Mn(CO)_5$ molecule. Keeping the structural parameters fixed at their experimental values, the total energy of the system has been determined as a function of the ϕ(HCMnC) dihedral angle, which describes the relative orientation of the CH_3 and

Table 2
Observed raman frequencies (cm^{-1}) of $CH_3Re(CO)_5$

Raman			Assignments [b]		
Solid 300 K	Solid 41 K	Solution (CH_2Cl_2)			
2963 m,b	2966 m,b	[a]	ν_{18}	e	CH str.
2905 s	2905 s	[a]	ν_1	a_1	CH str.
	2843 vw		$2\nu_{20}(2844)$	$A_1+B_1+B_2$	
2824 w	2826 w	2830 vw			
	2167 w				
2124 s	2125 s	2129 vs,p	ν_2	a_1	CO_e str.
2100 w	2100 vw	2103 vvw			
	2076 vvw		$\nu_3+\nu_{27}(2067)$	E	
2050 ms	2053 ms	2052 m,dp	ν_{12}	b_1	CO_e str. [c]
2039 vs	2038 vs				
1992 mw	1990 w	2010 vvw	ν_{19}	e	CO_e str.
1965 vw	1968 sh	1974 w,dp	ν_3	a_1	CO_a str. [c]
1951 m,b	1946 m				
1415 vvw	1422 vw		ν_{20}	e	CH_3 asym. def.
1189 m	1188 m		ν_4	a_1	CH_3 sym. def.
	1181 m		$2\nu_{13}(1178)$	A_1	
	1153 vw		$\nu_{16}+\nu_{22}(1135)$	E	
	1145 vvw				
1064 w	1057 vw		$\nu_6+\nu_{22}(1064)$	E	
960 vvw			$\nu_5+\nu_{24}(977)$	E	
868 vvw			$\nu_{23}+\nu_{24}(875)$	$A_1+B_1+B_2$	
772 w	776 w		ν_{21}	e	CH_3 rock.
748 w	750 vw	740 w,dp	$2\nu_{24}(760)$	$A_1+B_1+B_2$	
601 w	602 w	604 vvw	ν_5, ν_{22}	a_1, e	$ReCO_e$ bend., $ReCO_e$ bend.
589 w	587 w		ν_{13}	b_1	$ReCO_e$ ip. bend.
529 w	527 w	531 w	ν_{16}	b_2	$ReCO_e$ bend.
500 w	498 w	508 w	ν_{23}	e	$ReCO_a$ bend.
469 vs	472 vs	470 m,p	ν_6	a_1	Re–CO_a str.
448 s	450 vs	450 w,p	ν_7, ν_8	a_1, a_1	Re–CH_3 str., Re–CO_e str.
433 sh	430 w	430 sh	ν_{25}	e	Re-CO_e oop. def.
385 w,b	381 wsh	380 vw	ν_{24}	e	Re-CO_e str.
374 w,b	372 w				
	152 sh				
146 w	146 w		ν_{17}	b_2	CReC def.
106 vs	112 vs	100 m,dp	ν_{15}	b_1	CReC def.
96 m	93 sh		ν_9, ν_{27}	a_1, e	CReC def., CReC def.
[60]	[60]		ν_{28}	e	CreC def. [d]
48 vw	55 vw		Lattice mode		
(20)	(10)	(50)	Limit of study		

[a] Not observed, obscured by solvent bands.
[b] In parentheses, the calculated combination bands and overtones, based on the gas-phase frequencies.
[c] Multiple bands due to lattice splitting.
[d] Estimated frequencies.

$Mn(CO)_5$ units. The relative energies with respect to $\phi = 0$ are depicted in Fig. 2 and it reveals that all points lie in a very narrow energy range, in which they are somewhat randomly displaced. The random feature is due to the numerical uncertainty in the total energies associated with the incompleteness of the integration grid and therefore the conclusion one can draw from Fig. 2 is that the barrier of the CH_3 rotation is predicted to be less than 0.5 kcal mol^{-1} (which is in good accordance with the one calculated from the methyl rotation/torsion mode by Andrews et al.).

4.1. Force-field calculation

4.1.1. Metal–ligand force constants

No clear trend between the gas, solution and solid sample frequencies was always observed; therefore, the refined force constants are also not always decreasing in the order gas > solution > solid. Solid-state effects make it sometimes difficult to select the fundamental frequency value. Nevertheless, the carbonyl CO and M–CO stretching force constants follow the expected trend, but this is not the case for the diagonal deformation force constants (see Table 3). The CO stretching

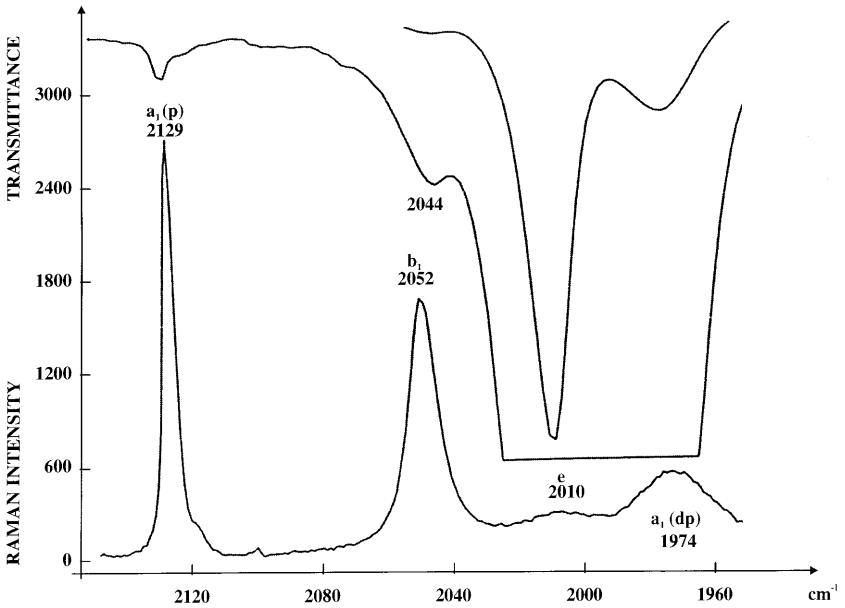

Fig. 1. Infrared and Raman spectra of $CH_3Re(CO)_5$ in CH_2Cl_2 solution in the range of CO stretching vibrations.

frequencies of the Mn and Re complex are practically identical (within 10 cm^{-1}). This is reflected by the rather similar CO stretching force constants as well. In contrast we see that the metal-ligand bondings are rather different.

The metal–ligand bonding force constants are increased by 10–25% for the Re complex as compared to those for the Mn molecule, indicating considerably stronger Re–CH_3 ($\sim$25%), Re–CO_e ($\sim$12%) and Re–CO_a ($\sim$10%) bonds (see Table 3). The metal–carbon stretching force constants for $Cr(CO)_6$ and $W(CO)_6$ have been reported as 2.08×10^2 and 2.32×10^2 Nm^{-1}, respectively [31]. The 13% difference for the $M(CO)_6$ species is almost identical with those for the $CH_3M(CO)_5$ metal–carbon stretching force constants (Table 4). In both cases, the greater metal–ligand π-bonding and the stronger M–C σ-bonding for the heavier metal (Re and W) are responsible for the larger force constants.

4.1.2. Carbonyl stretching force constants

From Table 4, it can be seen that substitution of a CO ligand in $M(CO)_6$ by a methyl group produces a significant difference in the axial CO and a moderate difference in the equatorial CO stretching force constants. The decreases of the force constants are likely attributed to an increase in the occupancy of the 2π levels of the CO ligand, and at the same time an increased donation from the 5σ level. The largely *trans*-directing effect of the ligand is similar to that noted for Br in $Mn(CO)_5Br$ [17]. The drastic differences between the metal–carbon stretching force constants for the axial/equatorial CO groups: 2.62/2.09, 2.61/2.30, and 2.94/2.61 $\times 10^2$ Nm^{-1} for $Mn(CO)_5Br$ [17], $CH_3Mn(CO)_5$ and $CH_3Re(CO)_5$, respectively, demonstrate the strong *trans*-influence of the ligand (Br, CH_3).

The stretch–stretch interaction force constants are also given in Table 4. In general, it can be concluded that the increasing positive charge on the central metal atom in the case of $M(CO)_5L$ listed in Table 4, and the strong metal–carbon bondings as compared to those of the relevant hexacarbonyls would lead to greater interaction terms of the CO stretches. The present normal-coordinate analysis, together with our earlier results [18], shows that the *trans*-interaction terms for metal pentacarbonyls are always larger than for the *cis* ones. In contrast to the different assumed relations between f^{c}_{ee} and f^{t}_{ee} and f_{ea} [17,35] we find that no general rule can be established, except that $f^{c}_{ee} \ll f^{t}_{ee}$. Any constraint for the CO stretching interaction force constants would

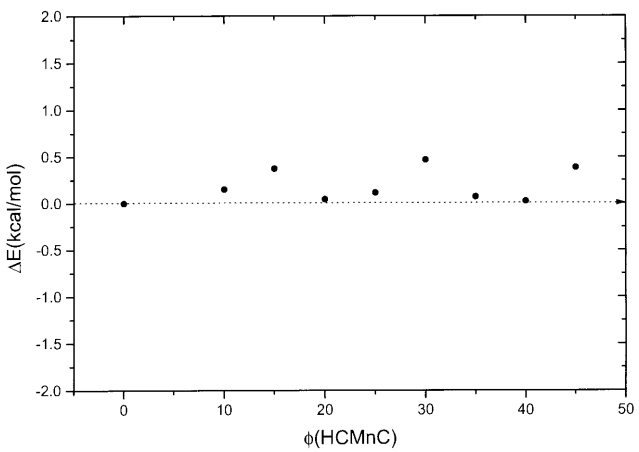

Fig. 2. Relative energies as a function of ϕ(HCMnC) dihedral angle as obtained from DFT calculations on $CH_3Mn(CO)_5$.

Table 3
Representative stretching force constants (10^2 Nm^{-1}) for $CH_3M(CO)_5$ (M = Mn(I), Re(I)) molecules

Force constant [a]	$CH_3Mn(CO)_5$			$CH_3Re(CO)_5$		
	Gas	Solution	Solid	Gas	Solution	Solid
Stretching						
$K(M–CH_3)$	1.506	1.506	1.609	1.876	1.969	1.890
$K(CO)_a$	16.362	16.156	15.848	16.158	16.002	15.913
$K(CO)_e$	17.004	16.880	16.776	17.035	16.829	16.653
$K(M–CO)_a$	2.712	2.612	2.568	3.035	2.936	3.007
$K(M–CO)_e$	2.315	2.299	2.297	2.542	2.612	2.514
Stretch–stretch						
$F(CO_e,CO_e)^c$	0.035	0.034	0.002	0.010	0.024	−0.033
$F(CO_e,CO_e)^t$	0.185	0.226	0.413	0.216	0.338	0.401
$F(CO_e,CO_a)$	0.202	0.202	0.202	0.240	0.240	0.240
$F(M–CO_e,M–CO_e)^c$	−0.030	−0.068	−0.033	0.148	0.121	0.114
$F(M–CO_e,M–CO_e)^t$	0.614	0.628	0.620	0.746	0.636	0.692
$F(M–CO_a,M–CO_e)$	−0.049	−0.025	0.024	0.021	0.025	0.024
$F(M–CO_a,MC)$	0.357	0.326	0.297	0.269	0.083	0.150

[a] Notes: $_a$, axial CO; $_e$, equatorial CO; ^{c}, *cis* CO,CO interaction; ^{t}, *trans* CO,CO interaction.

Table 4
Comparison of carbonyl stretching force constants (10^2 Nm^{-1}) among metal hexacarbonyls and related pentacarbonyls

Molecules	$K(CO)_a$ (f_a)	$K(CO)_e$ (f_e)	$F(CO_e,CO_e)^c$ (f^c_{ee})	$F(CO_e,CO_e)^t$ (f^t_{ee})	References, remarks
$Cr(CO)_6$	17.04	17.04	0.17	0.04	[31]
$[Cr(CO)_5CN]^-$	14.22	15.50	0.24	0.63	[18]
$[Mn(CO)_6]^+$	18.75	18.75	0.22	0.23	[a]
$CH_3Mn(CO)_5$	16.16	16.88	0.03	0.23	This work
$W(CO)_6$	17.22	17.22	0	0.22	[31]
$[W(CO)_5NCS]^-$	13.57	16.19	−0.09	1.11	[b]
$[Re(CO)_6]^+$	18.67	18.67	0.25	0.32	[c]
$CH_3Re(CO)_5$	16.00	16.83	0.02	0.34	This work

[a] Experimental frequencies from Ref. [32].
[b] Experimental frequencies from Ref. [33].
[c] Experimental frequencies from Ref. [34].

lead to very similar band separations of the CO stretching modes, especially the vibrations of the equatorial CO groups, in disagreement with the experimental observations. Since the CO groups are not coupled directly by kinematic elements, the CO,CO interaction force constants are largely responsible for the spectral distribution of the bands.

4.1.3. Methyl group force constants

In the field of structural chemistry, special attention has been paid to molecules forming σ-bonds between a transition metal and organic alkyl groups. The $CH_3Mn(CO)_5$ and $CH_3Re(CO)_5$ are good examples of this bonding interaction.

Throughout a complete series of molecules containing the CH_3–M group, the force field for this part remains rather constant. The metal–carbon stretching force constant (f_R) is the most sensitive to the type of metal and its oxidation state. Small changes in bond angle and bond length appear to have very little effect on the interaction force constants, but cause the diagonal constants to adjust. It appears therefore that a number of force constants can be transferred from molecule to molecule. These series of force fields for different methyl derivatives is given in Table 5 in internal coordinate representation (see Fig. 3). All four diagonal force constants, namely f_r, f_R, f_α and f_β have the highest values for hydrocarbons. It is interesting to note the changes in the force field that occur on replacing the terminal carbon atom by the other metal atom. As a consequence of experimental observations, methyl groups attached to different metals exhibit a remarkable frequency lowering of the CH stretching, CH_3 umbrella and rocking modes, which has the effect of decreasing f_r, f_α, and especially f_β force constants. One of the most important and very characteristic vibrations is the metal–carbon stretching mode. The strong increase of the f_R is due to the change of the oxidation state of the Re, from Re(I) in $CH_3Re(CO)_5$ to Re(VII) in the case of CH_3ReO_3 molecule.

Table 5
Comparison of methyl group force constants (10^2 Nm^{-1})

Force constant	$CH_3Mn(CO)_5$	$CH_3Re(CO)_5$	CH_3ReO_3 (Ref. [36])	CH_3–C (Ref. [37])	Units [a]
f_r [b]	4.78	4.71	4.78	4.86	a
f_{rr}	−0.04	−0.02	0.02	0.04	a
f_R	1.51	1.97	2.65	4.45 [c]	a
f_{rR}	−0.07	−0.07	0	0	a
f_α	0.52	0.53	0.47	0.55	b
f_β	0.42	0.43	0.30	0.64	b
$f_{\beta\beta}$	−0.03	−0.02	−0.15	−0.02	b
$f_{\alpha\beta}$	−0.02	−0.02	−0.08	−0.01	b
$f_{R\beta}$	−0.16	−0.29	−0.14	0.30	c
$f_{r\beta}$	0.16	0.16	−0.10	0.10	c
$f_{r\beta'}$	−0.06	−0.06	0	0	c

[a] Units: (a) 10^2 Nm^{-1}; (b) 10^{-18} Nm rad^{-2}; (c) 10^{-8} N rad^{-1}.
[b] For internal coordinates notation see Fig. 3.
[c] For C–C single bond.

4.2. Pressure effect

Micro-Raman spectra of crystalline $CH_3M(CO)_5$ (M = Mn, Re) have been recorded at selected pressures up to 40 kbar [11]. Both complexes showed pressure effects in the CO and M–CH_3 stretching regions indicating phase transition. It was interesting to know how the CO and M–CH_3 stretching force constants change as a function of pressure. In Fig. 4 the pressure dependence of axial and equatorial CO and different metal–carbon stretching force constants for $CH_3Mn(CO)_5$ and $CH_3Re(CO)_5$ are shown. The phase transition points are also clearly seen where the discontinuity occurs in the pressure/force constant plots.

The equatorial CO stretching force constant of $CH_3Mn(CO)_5$ is increasing from its original value 16.78×10^2 to 16.90×10^2 Nm^{-1} as the applied pressure is increased and the force constant versus pressure plot shows change in slope at the phase transition (~ 9 kbar). This accounts for the weakening of Mn–C(O) bonds in equatorial plane, e.g. to the expansion of $Mn(CO)_4$. The opposite effect has been observed for axial CO stretching at the low-pressure phase, when the CO bond is weakened, e.g. its original force constant 15.85×10^2 Nm^{-1} decreases to 15.72×10^2 Nm^{-1}, consequently the Mn–C(O) axial bond should be strengthened. After the phase transition (~ 9 kbar) the axial CO group shows similar behaviour as the equatorial ones with increasing external pressure.

In the low-pressure phase (below ~ 19 kbar) of $CH_3Re(CO)_5$ the equatorial CO stretching force constants exhibit general pressure dependence similar to those of $CH_3Mn(CO)_5$. The b_1 CO stretching mode (ν_{12}) appears as a doublet ($a_{1g} + b_{2g}$) in the Raman spectrum of the solid due to the lattice effect for the space group D_{2h} [16]. The frequency splittings of the ν_{12} mode are 2039 cm^{-1} (a_{1g}) and 2050 cm^{-1} (b_{2g}) at normal pressure and 2046 cm^{-1} (a_{1g}) and 2066 cm^{-1} (b_{2g}) at 40 kbar. The splitting of the $F_{12\ 12}$ (b_1) force constant increases from 0.18×10^2 to 0.33×10^2 Nm^{-1} due to the increased intermolecular interactions in the crystal lattice. This accounts for the compression of the unit cell and the separation of the intermolecular distances becomes smaller. Consequently the calculated CO stretching force constants at ambient pressure -0.023×10^2 Nm^{-1} increase at pressure close to phase transition to -0.043×10^2 Nm^{-1}. After the phase transition (~ 19 kbar) the correlation splitting becomes permanent.

At high pressures the pressure dependence of the axial CO stretching force constants for both molecules are significantly different. In the case of the Re compound it continues to be shifted to lower values (from 15.91 to 15.76×10^2 Nm^{-1}) with increasing pressure. This pressure effect completely agreed with increasing Re–C(O) axial force constant from 3.01×10^2 Nm^{-1} (at ambient pressure) towards 3.36×10^2 Nm^{-1} at 40 kbar.

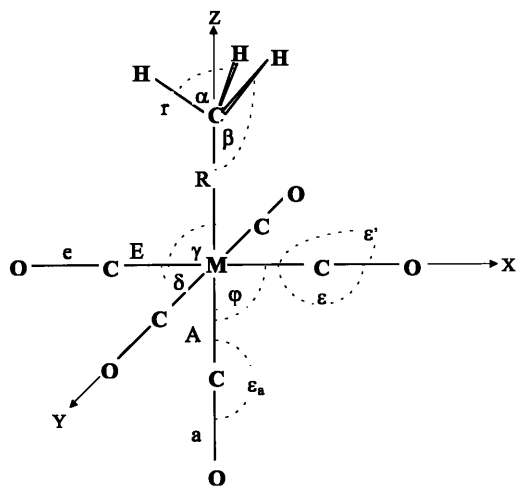

Fig. 3. Internal coordinates for $CH_3M(CO)_5$ (M = Mn, Re) molecules.

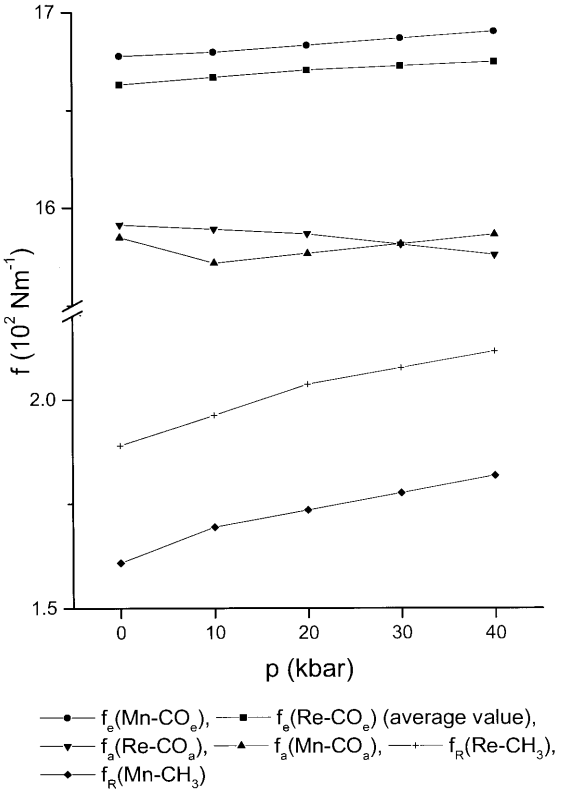

Fig. 4. Pressure dependence of equatorial and axial CO and M–CH_3 stretching force constants for $CH_3Mn(CO)_5$ and $CH_3Re(CO)_5$.

Similar pressure dependence has been observed for metal–methyl (M–C) force constants. Both Mn–C and Re–C bonds are strengthened with increasing pressure (Fig. 4).

For the pressure effect one can conclude that the equatorial metal–ligand bonds are expanded while axial metal–carbon bonds are compressed as a function of pressure with the exception of the Mn–CO axial bond which expands at high-pressure phase. The values calculated for the pressure sensitivities, df/dp in different phases can be interpreted as 'bond-compressibilities' for the coordinated carbonyl and methyl groups. The stronger bonds, having larger force constants should have a smaller pressure effect than the weaker ones. In this sense one can have 'elastic' bonds like axial metal–ligand bondings (df/dp is 0.85, 0.73 Nm^{-1} $kbar^{-1}$ for Mn–CH_3 and Re–CH_3, respectively) and 'rigid' bonds like CO bondings where the relative pressure effect is about 50% of the metal–carbon bonds.

5. Conclusions

The vibrational spectra of $CH_3Mn(CO)_5$ and $CH_3Re(CO)_5$ molecules in particular in the far-IR region have been reinvestigated. The complete Raman spectra (3500–50 cm^{-1}) of the Re compound both in solid phase and in CH_2Cl_2 solution have been presented for the first time. Slight modifications in the assignment have been proposed. Normal coordinate analyses have been performed using experimental data of different isotopic species for both complexes to evaluate force constants for gaseous, dissolved, and solid samples. The fitted diagonal force constants decreased in the following order: gas > solution > solid.

Density functional theory calculations were carried out in order to estimate the energy barrier of the CH_3 internal rotation in the Mn complex. The calculations showed that the potential barrier is less than 0.5 kcal mol^{-1}, which allows practically free rotation of the methyl group.

The study of pressure effect on CO and M–CH_3 stretching force constants showed that stronger bonds – like the COs – have a relatively smaller pressure effect than the weaker ones (M–CH_3). The calculated pressure sensitivities, df/dp can be interpreted as 'bond compressibilities' for the coordinated carbonyl and methyl groups.

Acknowledgements

This research was generously supported by operating and equipment grants from the following agencies: Hungarian Academy of Sciences (OTKA, T 025278 and T 016707, AKP 9793-2, 4/29), COST D-5 (Brussels), NSERC (Canada), and FCAR (Quebec). J.M. acknowledges NSERC (Canada) for the award of an International Collaborative Travel Grant that enabled him to do research at McGill University. We thank Bio-Rad (Germany) for financial support of the KK1 PhD project at the University of Veszprém.

References

[1] J.B. Wilford, F.G.A. Stone, Inorg. Chem. 4 (1965) 389.
[2] H.D. Kaesz, R. Bau, D. Hendrickson, J.M. Smith, J. Am. Chem. Soc. 89 (1967) 2844.
[3] F.A. Cotton, A. Musco, G. Yagupsky, Inorg. Chem. 6 (1967) 1357.
[4] R.W. Cattrall, R.J.H. Clark, J. Organomet. Chem. 6 (1966) 167.
[5] O. Kahn, M. Bigorgne, C. R. Acad. Sci. Ser. C 266 (1968) 792.
[6] W. Hieber, G. Braun, W. Beck, Chem. Ber. 93 (1960) 901.
[7] A.B. Dempster, D.B. Powell, N. Sheppard, J. Chem. Soc. A (1970) 1129.
[8] M.A. Andrews, J. Eckert, J.A. Goldstone, L. Passell, B. Swanson, J. Am. Chem. Soc. 105 (1983) 2262.
[9] C. Long, A.R. Morrisson, D.C. McKean, G.P. McQuillan, J. Am. Chem. Soc. 106 (1984) 7418.
[10] G.P. McQuillan, D.C. McKean, C. Long, A.R. Morrisson, I. Torto, J. Am. Chem. Soc. 108 (1986) 863.
[11] Y. Huang, I.S. Butler, D.F.R. Gilson, D. Lafleur, Inorg. Chem. 30 (1991) 117.
[12] D.J. Mafleur, M.Sc. Thesis, McGill University, Montreal, 1988.

[13] T.M. McHugh, A.J. Rest, J. Chem. Soc. Dalton Trans. (1980) 2323.
[14] I.S. Butler, D.F.R. Gilson, D. Lafleur, Appl. Spectrosc. 46 (1992) 1605.
[15] D. Lafleur, Y Huang, D.F.R. Gilson, I.S. Butler, J. Solid State Chem. 108 (1994) 99.
[16] J. Gang, M. Pennington, D.K. Russell, P.B. Davies, G.M. Hansford, N.A. Martin, J. Chem. Phys. 97 (1992) 3885.
[17] D.K. Ottesen, H.B. Gray, L.H. Jones, M. Goldblatt, Inorg. Chem. 12 (1973) 1051.
[18] J. Mink, W.P. Felhammer, K. Bar, unpublished results.
[19] H.M. Seip, R. Seip, Acta Chem. Scand. 24 (1970) 3431.
[20] D.W.H. Rankin, A. Robertson, J. Organomet. Chem. 105 (1976) 331.
[21] J. Mink, L.M. Mink, Computer Program System for Vibrational Analysis of Molecules, University of Erlangen, Erlangen, 1983.
[22] P.L. Goggin, G. Kemény, J. Mink, J. Chem. Soc. Faraday 72 (1976) 1025.
[23] A.D. Becke, Phys. Rev. A 38 (1988) 3098.
[24] J.P. Perdew, Phys. Rev. B 33 (1986) 8822 Erratum in: Phys. Rev. B 38 (1986) 7406.
[25] N. Godbout, J. Andzelm, D.R. Salahub, E. Wimmer, Can. J. Chem. 70 (1992) 560.
[26] F. Sim, D.R. Salahub, S. Chin, M. Dupuis, J. Chem. Phys. 95 (1991) 4317.
[27] D.R. Salahub, R. Fournier, P. Mlynarski, I. Pápai, A. St-Amant, J. Ushio, Density Functional Methods in Chemistry, Springer-Verlag, New York, 1991.
[28] A. St-Amant, Ph.D. Thesis, Université de Montréal, 1991.
[29] A. St-Amant, D.R. Salahub, Chem. Phys. Lett. 169 (1990) 387.
[30] I. Pápai, J. Chem. Phys. 103 (1995) 1860.
[31] L.H. Jones, R.S. McDowell, M. Goldblatt, Inorg. Chem. 8 (1969) 2349.
[32] R.A.N. McLean, Can. J. Chem. 52 (1974) 213.
[33] A. Wojcicki, M.F. Farona, J. Inorg. Nucl. Chem. 26 (1964) 2289.
[34] E.W. Abel, R.A.N. McLean, S.P. Tyfield, P.S. Braterman, A.P. Walker, J. Mol. Spectrosc. 30 (1969) 29.
[35] F.A. Cotton, C.S. Kraihanzel, J. Am. Chem. Soc. 84 (1962) 4432.
[36] J. Mink, G. Keresztury, A. Stirling, W.A. Herrmann, Spectrochim. Acta 50A (1994) 2039.
[37] J.L. Duncan, Spectrochim. Acta 20 (1964) 1197.